

This copy is for your personal, non-commercial use only.

If you wish to distribute this article to others, you can order high-quality copies for your colleagues, clients, or customers by [clicking here](#).

Permission to republish or repurpose articles or portions of articles can be obtained by following the guidelines [here](#).

The following resources related to this article are available online at www.sciencemag.org (this information is current as of August 9, 2011):

Updated information and services, including high-resolution figures, can be found in the online version of this article at:

<http://www.sciencemag.org/content/331/6019/906.full.html>

Supporting Online Material can be found at:

<http://www.sciencemag.org/content/suppl/2011/02/14/331.6019.906.DC1.html>

A list of selected additional articles on the Science Web sites **related to this article** can be found at:

<http://www.sciencemag.org/content/331/6019/906.full.html#related>

This article **cites 25 articles**, 6 of which can be accessed free:

<http://www.sciencemag.org/content/331/6019/906.full.html#ref-list-1>

This article has been **cited by** 1 articles hosted by HighWire Press; see:

<http://www.sciencemag.org/content/331/6019/906.full.html#related-urls>

This article appears in the following **subject collections**:

Anatomy, Morphology, Biomechanics

http://www.sciencemag.org/cgi/collection/anat_morp

previous work using classical oxygen isotope paleothermometry on conodont apatite from Anticosti and elsewhere (7) that reconstructed temperatures in the modern SST range for much of the Late Ordovician–Early Silurian except for cooling to ~24°C below and above the Lافramboise Member (7). These estimates assumed a constant $\delta^{18}\text{O}_{\text{water}}$ of -1.0‰; substituting our $\delta^{18}\text{O}_{\text{water}}$ values from the same units raises inferred temperatures by, on average, 8°C. Recent revision of the phosphate-water oxygen isotope fractionation equation (23) further suggests that all conodont-derived temperature estimates should be revised upward, bringing them into the range that we observe for the Late Ordovician–Early Silurian.

We cannot rule out the possibility that the trends we observe are influenced by changes in the basin hydrology of the Taconic Foreland, but, if they accurately reflect global trends in the tropical oceans, they imply a nonlinear relationship between tropical ocean temperatures and continental ice volumes (fig. S13A). This contrasts with expectations from climate simulations using a modern continental configuration and from proxy records of the past 60 million years (13) (fig. S13, B and C). Furthermore, coexistence of substantial south polar ice sheets with tropical SSTs regionally in excess of 30°C implies a steeper meridional temperature gradient than during other major glacial episodes (12, 24). Minor glaciations inferred to have occurred under high CO₂ conditions in the late Mesozoic–early Cenozoic (16, 25) may have exhibited similar

gradients but were comparatively short-lived. Both of these observations could plausibly be explained by nonlinear changes in the intensity of oceanic meridional overturning circulation (26), similar to those previously invoked to explain changes in the behavior of the Hirnantian carbon cycle (4, 5, 20). Although speculative, some support for this hypothesis is provided by the coincidence of our observed cooling pulse with the globally recognized Hirnantian positive carbon isotope excursion (5, 19, 20).

Lastly, by demonstrating that tropical cooling was largely limited to the Hirnantian Stage, our results support hypotheses linking the two-pulsed nature of the Late Ordovician mass extinction to rapid climate changes at the beginning and end of this interval (4, 20).

References and Notes

1. L. A. Frakes, J. E. Francis, J. I. Syktus, *Climate Modes of the Phanerozoic* (Cambridge Univ. Press, Cambridge, 1996).
2. A. Raymond, C. Metz, *J. Geol.* **112**, 655 (2004).
3. R. A. Berner, *Geochim. Cosmochim. Acta* **70**, 5653 (2006).
4. P. M. Sheehan, *Annu. Rev. Earth Planet. Sci.* **29**, 331 (2001).
5. P. J. Brenchley *et al.*, *Geology* **22**, 295 (1994).
6. D. P. Le Heron, J. A. Dowdeswell, *J. Geol. Soc. London* **166**, 277 (2009).
7. J. A. Trotter, I. S. Williams, C. R. Barnes, C. Lécuyer, R. S. Nicoll, *Science* **321**, 550 (2008).
8. J. D. Marshall, P. D. Middleton, *J. Geol. Soc. London* **147**, 1 (1990).
9. A. D. Herrmann, M. E. Patzkowsky, D. Pollard, *Palaeogeogr. Palaeoclimatol. Palaeoecol.* **206**, 59 (2004).
10. D. P. Schrag *et al.*, *Quat. Sci. Rev.* **21**, 331 (2002).
11. P. Ghosh *et al.*, *Geochim. Cosmochim. Acta* **70**, 1439 (2006).
12. R. E. Came *et al.*, *Nature* **449**, 198 (2007).

13. Materials and methods are available as supporting material on Science Online.
14. U. Brand, J. Veizer, *J. Sediment. Res.* **50**, 1219 (1981).
15. G. A. Shields *et al.*, *Geochim. Cosmochim. Acta* **67**, 2005 (2003).
16. A. Bornemann *et al.*, *Science* **319**, 189 (2008).
17. S. Schouten *et al.*, *Geology* **31**, 1069 (2003).
18. P. N. Pearson *et al.*, *Nature* **413**, 481 (2001).
19. A. Desrochers, C. Farley, A. Achab, E. Asselin, J. F. Riva, *Palaeogeogr. Palaeoclimatol. Palaeoecol.* **296**, 248 (2010).
20. P. J. Brenchley *et al.*, *Geol. Soc. Am. Bull.* **115**, 89 (2003).
21. L. Hints *et al.*, *Est. J. Earth Sci.* **59**, 1 (2010).
22. S. M. Savin, *Annu. Rev. Earth Planet. Sci.* **5**, 319 (1977).
23. E. Pucéat *et al.*, *Earth Planet. Sci. Lett.* **298**, 135 (2010).
24. MARGO Project Members, *Nat. Geosci.* **2**, 127 (2009).
25. A. Tripathi, J. Backman, H. Elderfield, P. Ferretti, *Nature* **436**, 341 (2005).
26. R. J. Stouffer, S. Manabe, *Clim. Dyn.* **20**, 759 (2003).
27. L. R. M. Coocks, T. H. Torsvik, *J. Geol. Soc. London* **159**, 631 (2002).
28. M. R. Saltzman, S. A. Young, *Geology* **33**, 109 (2005).
29. J. J. Sepkoski Jr., *Bull. Am. Paleontol.* **363**, 560 (2002).
30. We thank T. Raub, M. Rohrsen, and B. Gaines for assistance with field and lab work; D. Boulet and Société des établissements de plein air du Québec (SEPAQ) Anticosti for permission to work in Anticosti National Park; and B. Hunda for supplying samples. This work was funded by an Agouron Institute award to W.W.F. and D.A.F. and NSF Division of Earth Sciences awards to W.W.F. and J.M.E.

Supporting Online Material

www.sciencemag.org/cgi/content/full/science.1200803/DC1

Materials and Methods

Figs. S1 to S13

Table S1

References

23 November 2010; accepted 19 January 2011

Published online 27 January 2011;

10.1126/science.1200803

Hibernation in Black Bears: Independence of Metabolic Suppression from Body Temperature

Øivind Tøien,^{1*} John Blake,¹ Dale M. Edgar,^{2†} Dennis A. Grahn,³ H. Craig Heller,³ Brian M. Barnes^{1*}

Black bears hibernate for 5 to 7 months a year and, during this time, do not eat, drink, urinate, or defecate. We measured metabolic rate and body temperature in hibernating black bears and found that they suppress metabolism to 25% of basal rates while regulating body temperature from 30° to 36°C, in multiday cycles. Heart rates were reduced from 55 to as few as 9 beats per minute, with profound sinus arrhythmia. After returning to normal body temperature and emerging from dens, bears maintained a reduced metabolic rate for up to 3 weeks. The pronounced reduction and delayed recovery of metabolic rate in hibernating bears suggest that the majority of metabolic suppression during hibernation is independent of lowered body temperature.

Mammalian hibernation is well characterized in species such as marmots, ground squirrels, bats, and dasyurid marsupials (1). These small (<5 kg) hibernators undergo regulated decreases in core body temperature (T_b) to near or below freezing during torpor bouts that last days to weeks (2–5). Torpor is periodically interrupted by arousals to normothermia (35° to 38°C) that usually last for less than one day (6, 7). During torpor, metabolic rates of small

hibernators decrease to 2 to 5% of basal metabolic rate (BMR) (8–10). However, the relative contributions of temperature-dependent (described by Q_{10} , rate coefficient for a 10°C change in T_b) and temperature-independent mechanisms of metabolic suppression depend on the size of animals and stage of entry into torpor (11). In contrast, the relationships between T_b and metabolism in the large hibernators of the bear family Ursidae have remained unknown because technical lim-

itations have prevented continuous, long-term monitoring in these 30 to 200 kg or larger animals. We used telemetry and respirometry to record T_b , metabolic rates, and heartbeat patterns of black bears, *Ursus americanus*, through their hibernation and post-hibernation recovery.

Black bears were nuisance animals captured in south-central or interior Alaska in late autumn 3 different years and transported to facilities at the Institute of Arctic Biology, University of Alaska Fairbanks. Radio transmitters for T_b and electromyogram (EMG)/electrocardiogram (ECG) were surgically implanted (12), and animals were transferred to outdoor enclosures in an isolated wooded area. Bears hibernated inside 0.8 m³ wooden nest boxes with straw for bedding and equipped with infrared cameras, activity detectors, and telemetry-receiving antennas. Food and water were not provided. Air was continuously collected from the closed hibernacula to record O₂ consumption (a measure of metabolic rate). After

¹Institute of Arctic Biology, University of Alaska Fairbanks, Fairbanks, AK 99775, USA. ²Department of Psychiatry and Behavioral Sciences, School of Medicine, Stanford University, CA 94305, USA. ³Department of Biological Sciences, Stanford University, CA 94305, USA.

*To whom correspondence should be addressed. E-mail: otoienv@alaska.edu (O.T.); bmbarnes@alaska.edu (B.M.B.)

†Present address: Lilly Research Centre, Eli Lilly, Windlesham, Surrey, GU20 6PH, UK.

the spontaneous emergence of bears from their dens in spring, T_b recordings were continued, and minimum metabolism after 24 hours of fasting was determined every four nights for 1 month.

Hibernating black bears kept a curled posture (Fig. 1), similar to that previously described (13), that facilitates heat preservation and water economy. Animals changed position twice a day to once every 2 days, when they stood, occasionally groomed, and rearranged bedding material. T_b , which is normally 37° to 38°C, decreased to average levels of 33.0°C (31.7° to 34.0°C, $n = 4$ bears) in mid hibernation (defined as 21 January to 20 February). Minimum T_b was 30.4°C (29.4° to 32.5°C, $n = 4$ bears). Before emergence in mid-April, T_b gradually increased over 2 to 4 weeks to 36° to 37°C (Fig. 2). Hibernating bears did not show spontaneous, periodical arousals to normothermic levels of T_b , as do small hibernators. This may be because bear T_b did not decrease below 30°C, a level that may reflect a threshold below which neural deficits, such as loss of neuronal structure (14), begin to occur that require regular returns to high T_b . Hibernating fat-tailed dwarf lemurs that are regularly warmed by the sun to above 30°C also do not show spontaneous arousals (15). Diurnal rhythms in T_b also were not evident in mid-winter; instead, there were unexpected 1.6- to 7.3-day cycles of T_b with 2° to 6°C amplitude. Cycles were shortest during coldest conditions and most regular in the smallest bear (Fig. 2B, top). T_b was higher and more stable in free-ranging black bears studied in Wyoming and Colorado, which could be due to milder ambient temperatures (16). In spring when conditions were warmer in our study, multi-day T_b cycles were also less evident (Fig. 2). High-amplitude multi-day cycles of T_b may be a feature of thermoregulation, when gradients between T_b and environmental temperatures are large. Early studies on hibernating black bears in Alaska or arctic Canada reported T_b of 32° to 35°C (17, 18) and could not reveal any multi-day patterns because of intermittent measurements.

The T_b of a female bear remained at normothermic levels through the end of January (Fig. 2C, bottom), when she gave birth to a 243-g cub that died because of a congenital diaphragmatic hernia (12). Afterwards, her T_b became more variable and decreased toward levels of other

hibernating bears. High and stable T_b patterns occurred during pregnancy in a European brown bear (19). Bears have delayed implantation, and pregnancy starts in late November after denning (20). We suggest that low and fluctuating T_b may not be favorable for embryonic development, and thus, hibernating bears maintain normothermia while pregnant.

O₂ consumption in hibernating bears varied from minimum levels of 0.06 ml g⁻¹ h⁻¹ sustained for as much as one day to brief peaks of >0.35 ml g⁻¹ h⁻¹ accompanied by movement (Fig. 3A). T_b declined when metabolism and shivering were minimal and increased during intense shivering and heightened metabolism. This varying pattern of endothermic thermoregulation

can explain the wide range in metabolic rates found in the only previous metabolic study of hibernating bears (18). Predicted BMR for carnivores (21, 22) averages 0.228 ml g⁻¹ h⁻¹. Here, we show BMR (defined as overnight resting and fasting metabolic rate measured 1 month after emergence from hibernation) was 0.276 ml g⁻¹ h⁻¹ (range from 0.267 to 0.285 ml g⁻¹ h⁻¹, $n = 3$ bears); the mean T_b was 37.8°C. A comparison of the changes in metabolism and corresponding T_b in three nonpregnant bears (Fig. 3B) revealed that during mid-hibernation, when T_b was 32.2°C (30.9° to 33.6°C), minimum metabolic rate (12) was 0.069 (0.056 to 0.086) ml g⁻¹ h⁻¹, or 24.9% of BMR. A reduction to only 0.179 ml g⁻¹ h⁻¹ (64.9% of BMR) would be expected because of

Fig. 2. Body temperature patterns of hibernating black bears. Core body temperature (T_b , black), temperature outside dens (T_a , blue), and movements (purple) recorded over 3 different years. (A) One bear. (B) Two bears. (C) Two bears. Female BB99-02F was pregnant and gave birth, indicated by the plus symbol. Implantation of T_b transmitters in (C) occurred before the EMG/ECG transmitter surgery, marked by an asterisk. Surgery (both transmitters) for the other bears took place simultaneously and before recording. Missing T_b data for BB92-01M were due to instrumentation problems.

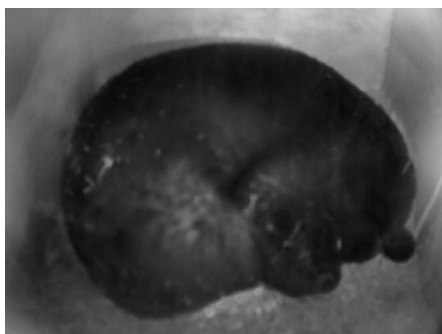
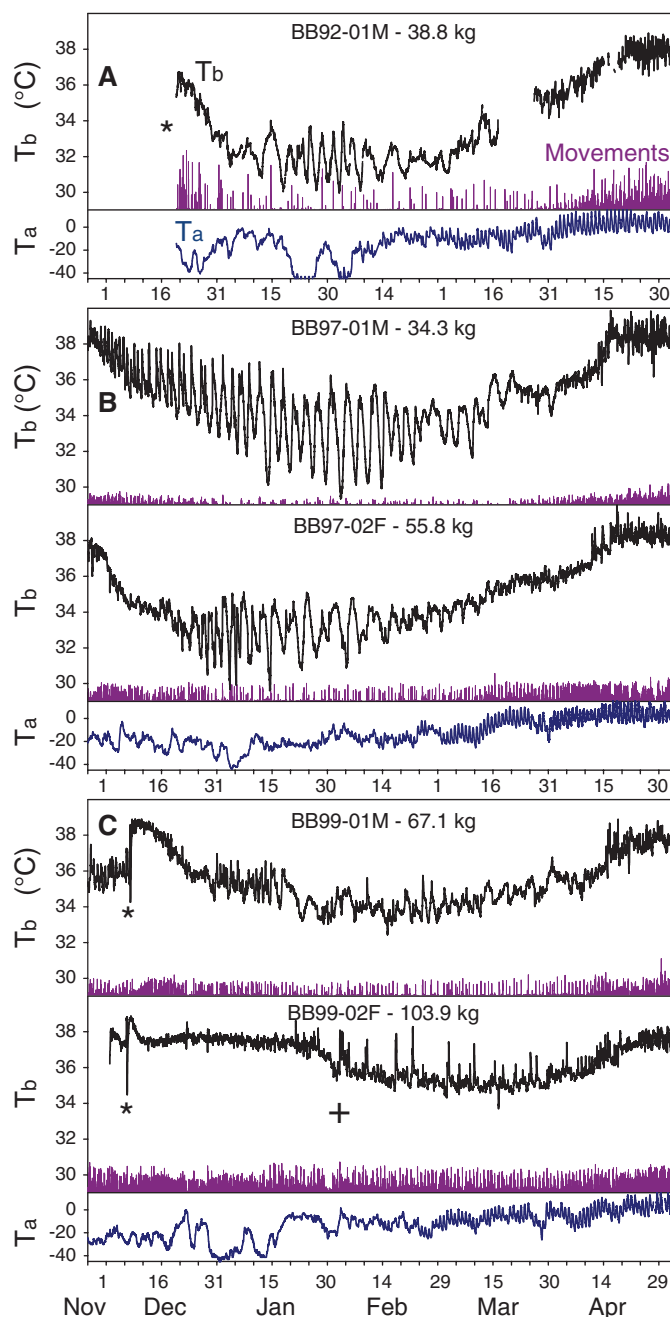


Fig. 1. Black bear hibernating in its artificial den.

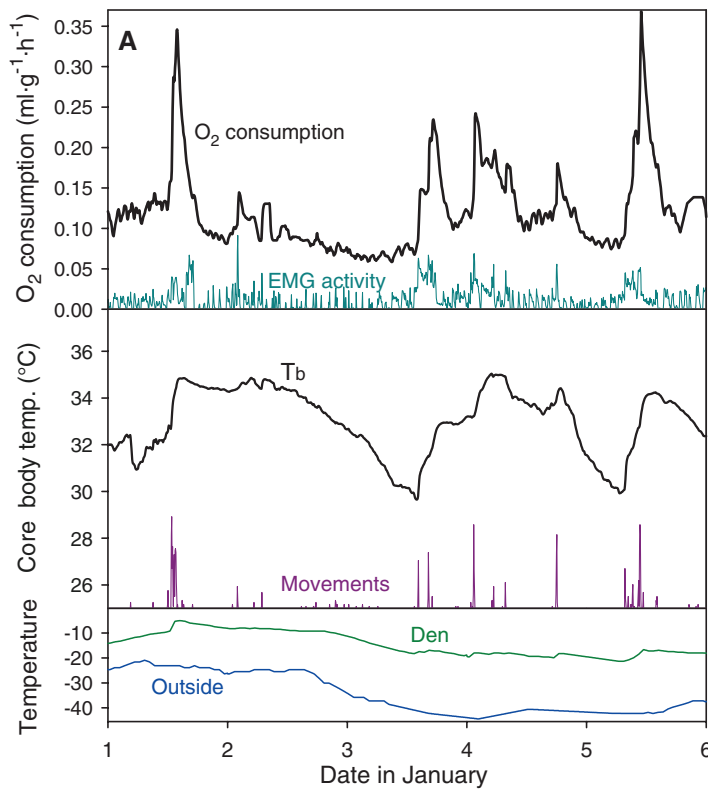
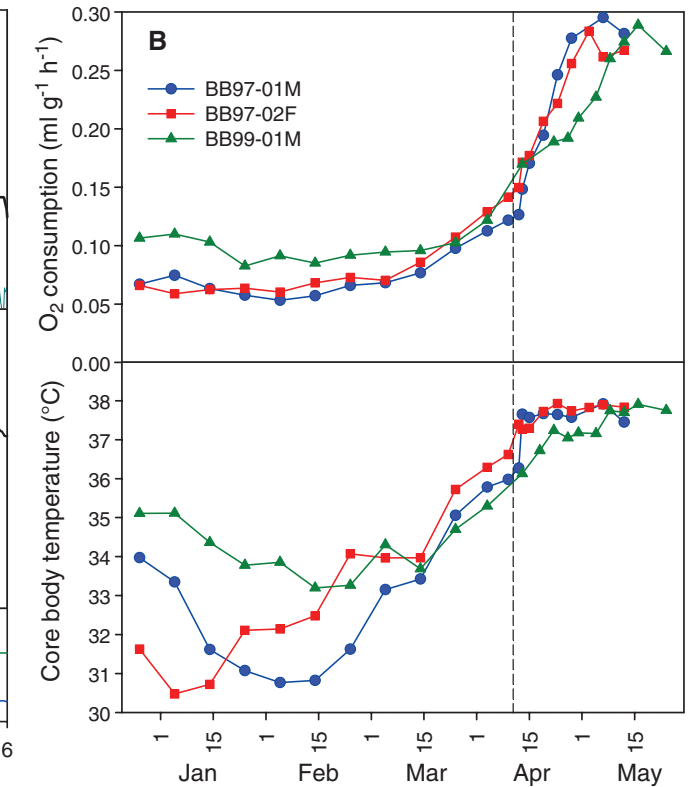


Fig. 3. Body temperature and metabolic rate of hibernating black bears. **(A)** O_2 consumption, EMG activity, T_b , movements, and temperature outside and inside the den of BB97-02F during a 5-day period in January. **(B)** Minimum O_2



consumption and corresponding T_b of three bears during hibernation and during recovery from hibernation. The vertical dashed line indicates the average time of emergence, which varied by ± 2 days.

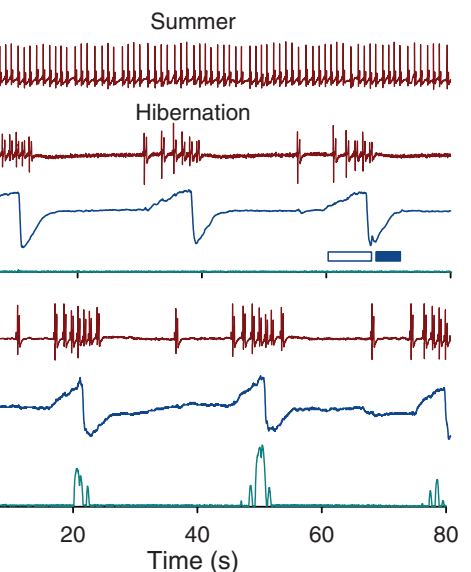
direct effects of the 5.5°C decrease in T_b , when a Q_{10} of 2.2 is assumed (1). When bears emerged from dens in mid-April with T_b of 36.6°C (36.1° to 37.4°C), metabolic rate averaged 0.149 (0.127 to 0.170) $\text{ml g}^{-1} \text{h}^{-1}$ or 52.9% of BMR and stabilized at BMR levels after 2 to 3 weeks (Fig. 3B). Bears began feeding over this period, and their return to BMR may in part involve resumption of a full capacity of the digestive system. In alpine marmots, hibernation is accompanied by a 70% decrease in mass of stomach and intestines, which was reversed in spring (23). Hypothyroidism of hypothalamic origin reported in hibernating black bears (24) may also contribute to metabolic suppression.

Decreased metabolism in hibernating bears reduces the need for transport of blood gases and nutrients. Heart rate (HR) of three non-pregnant bears in mid-hibernation decreased from summer resting levels (Fig. 4A) of 55 (44.5 to 63.7) beats per min to 14.4 (8.9 to 20.1) beats per min, which is similar to minima of 8 to 12 beats per min in a captive hibernating black bear reported by Folk (25). Hibernating bears showed a marked variation in inter-beat intervals through the breathing cycle, encompassing a profound sinus arrhythmia (Fig. 4, B and C). Typically, a group of rapid heartbeats occurred as inspiration ended followed by interbeat intervals of 8 to 20 s after expiration. Bursts of shivering were synchronous with rapid heartbeats and breathing (Fig. 4C). At emer-

Fig. 4. ECG and breathing patterns in summer and hibernating bears. **(A)** Representative ECG for a bear in summer. **(B and C)** ECG, breathing (chamber pressure), and EMG amplitude of two hibernating bears, **(B)** BB99-01M and **(C)** BB97-02F, showing increased heart rate at inspiration. The open bar marks inspiration, and the filled blue bar marks expiration. The peaks in average EMG amplitude in **(C)** are shivering bursts, which occurred at the end of inspiration.

gence, sinus arrhythmia was less pronounced, and average resting HR was 23.7 (16.1 to 31.1) beats per min. HR during hibernation was reduced to 26.2% and at emergence was 43.0% of summer levels. Similar reductions in HR during hibernation with a transition at emergence have been observed in grizzly bears (26).

Black bears share attributes of hibernation with small hibernators, including a decrease in



metabolic rate, lack of diurnal T_b patterns, reduced HR, and surviving without feeding or drinking for approximately half a year. However, T_b in hibernating bears is far higher than in small hibernators, which is in part due to the estimated lower levels of thermal conductance in bears (approximately 20%) as compared with ground squirrels [supporting online material (SOM) text and table S1] (10). Whereas smaller hibernators

show long torpor bouts interrupted by regular arousal episodes, black bears in Alaska exhibit distinct cyclic non-diurnal T_b patterns. Bear metabolism is reduced by 53% from BMR, even when T_b has returned to normothermic levels. These observations expand the phenotype of mammalian hibernation that occurs in diverse animals over body mass ranges from 0.005 to 200 kg. Insights into how hibernating bears achieve and cope with these reductions in energy need and T_b , as well as conservation of muscle (27, 28) and bone mass (29) despite prolonged seasonal inactivity and disuse, could lead to the development of novel clinical therapies. Current molecular and genetic approaches (28, 30) in combination with better physiological knowledge can increase our understanding of the regulation of hibernation in small and large hibernators and their evolution.

References and Notes

1. F. Geiser, *Annu. Rev. Physiol.* **66**, 239 (2004).
2. H. C. Heller, G. W. Colliver, *Am. J. Physiol.* **227**, 583 (1974).
3. G. L. Florant, H. C. Heller, *Am. J. Physiol.* **232**, R203 (1977).
4. B. M. Barnes, *Science* **244**, 1593 (1989).
5. F. Geiser, T. Ruf, *Physiol. Zool.* **68**, 935 (1995).
6. C. P. Lyman, J. S. Willis, A. Malan, L. C. H. Wang, *Hibernation and Torpor in Mammals and Birds* (Academic Press, New York, 1982).
7. T. N. Lee, B. M. Barnes, C. L. Buck, *Ethol. Ecol. Evol.* **21**, 403 (2009).
8. B. D. Snapp, H. C. Heller, *Physiol. Zool.* **54**, 297 (1981).
9. G. Heldmaier, T. Ruf, *J. Comp. Physiol. B* **162**, 696 (1992).
10. C. L. Buck, B. M. Barnes, *Am. J. Physiol.* **279**, R255 (2000).
11. F. Geiser, *J. Comp. Physiol. B* **158**, 25 (1988).
12. Materials and methods are available as supporting material on Science Online.
13. G. E. Jr, Folk, J. M. Hunt, M. A. Folk, in *Bears—Their Biology and Management*, C. J. Martinka, K. L. McArthur, Eds. (Bear Biology Association, Tonto Basin, AZ, 1980), pp. 43–47.
14. C. G. von der Ohe, C. C. Garner, C. Darian-Smith, H. C. Heller, *J. Neurosci.* **27**, 84 (2007).
15. K. H. Dausmann, J. Glos, J. U. Ganzhorn, G. Heldmaier, *Nature* **429**, 825 (2004).
16. H. J. Harlow, T. Lohuis, R. C. Anderson-Sprecher, T. D. I. Beck, *J. Mammal.* **85**, 414 (2004).
17. R. J. Hock, *2nd Alaskan Sci. Conf., AAAS* **2**, 310 (1951).
18. P. D. Watts, C. Cuyler, *Acta Physiol. Scand.* **134**, 149 (1988).
19. R. Hissa, *Ann. Zool. Fenn.* **34**, 267 (1997).
20. R. L. Rausch, *Z. Säugetierkd.* **26**, 65 (1961).
21. V. Hayssen, R. C. Lacy, *Comp. Biochem. Physiol. A* **81**, 741 (1985).
22. B. K. McNab, *Comp. Biochem. Physiol. A* **151**, 5 (2008).
23. I. Hume *et al.*, *J. Comp. Physiol. B* **172**, 197 (2002).
24. F. Azzì, J. E. Mannix, D. Howard, R. A. Nelson, *Am. J. Physiol.* **237**, E227 (1979).

25. G. E. Jr, Folk, in *Mammalian Hibernation*, vol. III, K. Fisher, A. R. Dawe, C. P. Lyman, Schönbaum, F. E. Jr. South, Eds. (Oliver & Boyd, Edinburgh, Scotland, 1967), pp. 75–85.
26. O. L. Nelson, C. T. Robbins, *J. Comp. Physiol. B* **180**, 465 (2010).
27. H. J. Harlow, T. Lohuis, T. D. I. Beck, P. A. Iaizzo, *Nature* **409**, 997 (2001).
28. V. B. Fedorov *et al.*, *Physiol. Genomics* **37**, 108 (2009).
29. S. W. Donahue, M. R. Vaughan, L. M. Demers, H. J. Donahue, *J. Exp. Biol.* **206**, 4233 (2003).
30. C. Shao *et al.*, *Mol. Cell. Proteomics* **9**, 313 (2010).
31. This work was supported by U.S. Army Medical Research and Materiel Command grant 05178001; NSF grants 9819540, 0076039, and 0732755; NIH HD-00973; and gift funds to Stanford University, American Heart Association #0020626Z, and the Fulbright Program. We thank the Alaska Department of Fish and Game for providing bears, D. Ritter for technical assistance, and J. Kenagy and J. Duman for comments.

Supporting Online Material

www.sciencemag.org/cgi/content/full/331/6019/906/DC1
Materials and Methods
SOM Text
Table S1
References

22 October 2010; accepted 13 January 2011
10.1126/science.1199435

LysM-Type Mycorrhizal Receptor Recruited for Rhizobium Symbiosis in Nonlegume *Parasponia*

Rik Op den Camp,¹ Arend Streng,¹ Stéphane De Mita,^{1*} Qingqin Cao,^{1†} Elisa Polone,^{1,2} Wei Liu,^{1,3} Jetty S. S. Ammiraju,⁴ Dave Kudrna, Rod Wing,⁴ Andreas Untergasser,^{1‡} Ton Bisseling,^{1,5§} René Geurts¹

Rhizobium–root nodule symbiosis is generally considered to be unique for legumes. However, there is one exception, and that is *Parasponia*. In this nonlegume, the rhizobial nodule symbiosis evolved independently and is, as in legumes, induced by rhizobium Nod factors. We used *Parasponia andersonii* to identify genetic constraints underlying evolution of Nod factor signaling. Part of the signaling cascade, downstream of Nod factor perception, has been recruited from the more-ancient arbuscular endomycorrhizal symbiosis. However, legume Nod factor receptors that activate this common signaling pathway are not essential for arbuscular endomycorrhizae. Here, we show that in *Parasponia* a single Nod factor–like receptor is indispensable for both symbiotic interactions. Therefore, we conclude that the Nod factor perception mechanism also is recruited from the widespread endomycorrhizal symbiosis.

The rhizobial nodule symbiosis is widespread in the legume family (Fabaceae). Although this nitrogen-fixing symbiosis provides the plant with a major advantage, it is in principle restricted to a single family, and it is a major challenge for future agriculture to transfer this symbiosis to nonlegumes (1). The genus *Parasponia* could provide a key to this, because it encompasses the only nonlegume species that acquired also the rhizobium symbiosis (2, 3), where “rhizobium” refers to all species and genera that form nodules on legumes. *Parasponia* comprises several tropical tree species and belongs to Celtidaceae (4). Celtidaceae (order Rosales) and Fabaceae (order Fabales) are only remotely related.

Further, not a single species phylogenetically positioned between *Parasponia* and Fabaceae is able to establish such rhizobium symbiosis. Hence, in all probability the common ancestor of present *Parasponia* species gained the rhizobium–nodule symbiosis independent from legumes. Therefore, a legume–*Parasponia* comparison provides a key to identifying genetic constraints underlying this symbiosis. In this study, we focused on parallel evolution of the recognition of the rhizobial signal that starts the symbiotic interaction, the Nod factor.

Parasponia makes lateral rootlike nodules that are associated with cell divisions in the root cortex (5). Rhizobium enters the *Parasponia* root intercellularly and becomes imbedded in a dense

matrix. Rhizobium obtains an intracellular life-style when it reaches a nodule primordium. There, cortical cells are infected via threadlike structures that remain connected to the plasma membrane. These so-called fixation threads branch, fill up the cells, and provide a niche to rhizobia to fix nitrogen (5). This is illustrated by the expression, in these threads, of the rhizobium *nifH* gene that encodes one of the subunits of nitrogenase (fig. S1). In contrast, rhizobia enter most legume roots via root hair–based intracellular infection threads, and the bacteria are released in nodule cells as membrane-surrounded nitrogen-fixing organelle-like structures (symbiosomes) that harbor a single or only a few bacteria. Legume nodules are considered to be genuine organs with a unique ontogeny (6). The fact that the *Rhizobium* symbiosis is very common in 65-million-year-old Fabaceae led to the conclusion that the symbiotic

¹Department of Plant Sciences, Laboratory of Molecular Biology, Wageningen University, Droevendaalsesteeg 1, 6708 PB Wageningen, Netherlands. ²Department of Agricultural Biotechnologies, Università di Padova, Viale dell'Università 16, 35020 Legnaro (Padova), Italy. ³Key Laboratory of Molecular and Developmental Biology, Institute of Genetics and Developmental Biology, Chinese Academy of Sciences, Beijing 100101, China. ⁴University of Arizona, Plant Sciences Department, 303 Forbes Building, Tucson, AZ 85721-0036, USA. ⁵College of Science, King Saud University, Post Office Box 2455, Riyadh 11451, Saudi Arabia.

*Present address: Institut de Recherche pour le Développement Montpellier, 911 Avenue, Agropolis BP 64501, 34394 Montpellier, cedex 5, France.

†Present address: Department of Biotechnology, Beijing University of Agriculture, No. 7 Beinong Road, Huilongguan Changping District, Beijing, People's Republic of China.

‡Present address: Zentrum für Molekulare Biologie der Universität Heidelberg, Im Neuenheimer Feld 282, 69120 Heidelberg, Germany.

§To whom correspondence should be addressed. E-mail: ton.bisseling@wur.nl